Available online at www.sciencedirect.com
ScienceDirect
Journal of Physics and Chemistry of Solids 69 (2008) 2019–2024
JOURNAL OF PHYSICS AND CHEMISTRY OF SOLIDS
www.elsevier.com/locate/jpcs

Optimization on technical parameters for fabrication of SDC film by screen-printing used as electrolyte in IT-SOFC

Lijun Zhao[a], Xiqiang Huang[a,*], Ruibin Zhu[a], Zhe Lu[a], Weiwei Sun[a,b], Yaohui Zhang[a], Xiaodong Ge[a], Zhiguo Liu[a], Wenhui Su[a,c]

[a]*Center for Condensed Matter Science and Technology, Harbin Institute of Technology, Harbin 150001, China*
[b]*College of Natural Sciences, Jiamusi University, Jiamusi 154007, China*
[c]*International Center for Material Physics, Academia, Shenyang 110015, China*

Received 14 December 2007; received in revised form 14 February 2008; accepted 18 February 2008

Abstract

Sm-doped Ceria (SDC) electrolyte film was successfully fabricated on anode substrate of NiO-SDC by screen-printing. Some technical parameters for fabrication were investigated and optimized, including printing times, ink composition and sintering temperature. Scanning electron microscope (SEM) measurement was done to check the microstructures of SDC film and single cell. The parameters greatly affected the quality of SDC film and cell performance. The single cell with the optimum parameters exhibited an OCV of 0.82 V and a power density of 0.5 W/cm^2 at 600 °C.

Keywords: A. Thin films; D. Electrochemical properties; D. Microstructure

1. Introduction

Solid oxide fuel cell (SOFC) has attracted more and more attention, due to its advantages: cleanliness, efficiency, low pollution and fuel flexibility [1]. For long-life working and encouraging its practical application, many research groups focused their study on reducing the operation temperature of SOFC [2–10]. Recently, CeO_2-based oxide, such as Sm-doped Ceria (SDC) [2,4–6] and Gd-doped Ceria (CGO) [3,10], was frequently used as electrolyte for IT-SOFC (intermediate temperature SOFC), due to their high oxide-ionic conductivity compared to Y_2O_3-stabilized ZrO_2 (YSZ) in the intermediate-temperature range. Furthermore, thermal expansion coefficient ($12.5 \times 10^{-6} K^{-1}$) of doped Ceria is much closer to that of Ni-based substrate, compared with YSZ ($10.5 \times 10^{-6} K^{-1}$) [2].

For further improving cell performance, it is necessary to reduce the thickness of electrolyte to lower ohmic loss. Some research groups focused on techniques to fabricate electrolyte film, including slurry coating [3], spary pyrolysis [10], pulsed laser deposition [10], electrophoretic deposition [5,11], dry pressing [6,12,13], tape-casting [2,14], chemical vapor deposition (CVD) [15], DC magnetron sputtering [16], sol–gel dip-drawing [17], spray coating [18,19], plaster casting [20], slurry spin coating [21,22], screen-printing [23–25], and so on. Compared with the other techniques, screen-printing is low-cost, easy to realize, and suitable for mass-production. In the screen-printing processing, many technical parameters can greatly affect the quality of electrolyte film and the fabrication reproducibility. However, to our knowledge, there is hardly any report on optimizing the parameters.

In this paper, effects of some technical parameters on SDC electrolyte film and cell performance were investigated and the parameters were optimized.

2. Experimental

NiO powder was prepared by a precipitation method. $Ba_{0.5}Sr_{0.5}Co_{0.8}Fe_{0.2}O_{3-\delta}$ (BSCF) powder was synthesized by a citric–nitrate process, and SDC ($Sm_{0.2}Ce_{0.8}O_{1.9}$)

*Corresponding author. Tel.: +86 451 86418420; fax: +86 451 86412828.
E-mail address: huangxq@hit.edu.cn (X. Huang).

0022-3697/$ - see front matter © 2008 Elsevier Ltd. All rights reserved.
doi:10.1016/j.jpcs.2008.02.011

powder as well. Ammonia and $Ni(NO_3)_2 \cdot H_2O$, $Ba(NO_3)_2$, $Sr(NO_3)_2$, $Co(NO_3)_2 \cdot 6H_2O$, $Fe(NO_3)_3 \cdot 9H_2O$, $Ce(NO_3)_3 \cdot 6H_2O$, and Sm_2O_3 used as raw materials, were all analytical reagent (A.R.). Please see Ref. [24] for detailed information on the preparation process of NiO, BSCF and SDC powder. The as-prepared NiO and SDC powder was mixed in a weight ratio of 65:35 and ball-milled for 10 h with ethanol as media. 15 wt% starch was added as pore former. Then the mixed powder was pressed into pellets of 13 mm in diameter and 0.5 mm in thickness. After being sintered at 1000 °C for 2 h, the pellets can be used as substrates for the screen-printing processing.

Ink for screen-printing was composed of x wt% SDC power and $100-x$ wt% ($x = 30$, 40, 50 and 60) ethyl cellulose–terpineol vehicle. A terylene screen was used with mesh count of 165 wires cm^{-1} and wire-diameter of 30 μm. The screen had an opening size of 30 μm and an open area of 25%. One printing pass was done during one-time printing process. Between two printing processes, the printed film was dried in air at room temperature for about 15 min. Different printing times (one-, three-, five and seven-time) were employed to get green SDC films, which were then sintered at different temperatures (1300, 1350, 1400 and 1450 °C) for 4 h with a heating rate of 5 °C min^{-1}. Then the BSCF powder was screen-printed onto the surface of SDC films, and sintered at 970 °C for 3 h to obtain BSCF cathode.

The microstructures of the SDC films and single cells was examined by a scanning electron microscope (SEM). Solartron SI 1260 impedance/grain-phase analyzer in combination with SI 1287 electrochemical interface was employed to measure the cell performance with a four-probe method. Hydrogen and air was used as fuel and oxidant, respectively.

3. Results and discussion

3.1. Effect of printing times

3.1.1. SEM

SEM result for the surface view and cross-sectional view of SDC films with different printing times was shown in Fig. 1. It was seen from the surface view that the number of holes in SDC film decreased with the increase of printing times. The SDC film fabricated by a seven-time printing processing exhibited a densest structure.

As shown in the cross-sectional images in Fig. 1, thickness of SDC film increased with the printing times. The linear dependence of the thickness of SDC film on the printing times was plotted in Fig. 2. As shown in Fig. 2, every two-time printing processing resulted in a 4.5 μm increase of the thickness of SDC film. The thickness of SDC film fabricated by a seven-time printing processing was about 16.5 μm.

3.1.2. Cell performance

As many researchers reported [2–4,6,26,27], single cell with SDC electrolyte usually shows an OCV of only about 0.8 V, which was lower than the theoretical value due to the low ionic transport number of SDC.

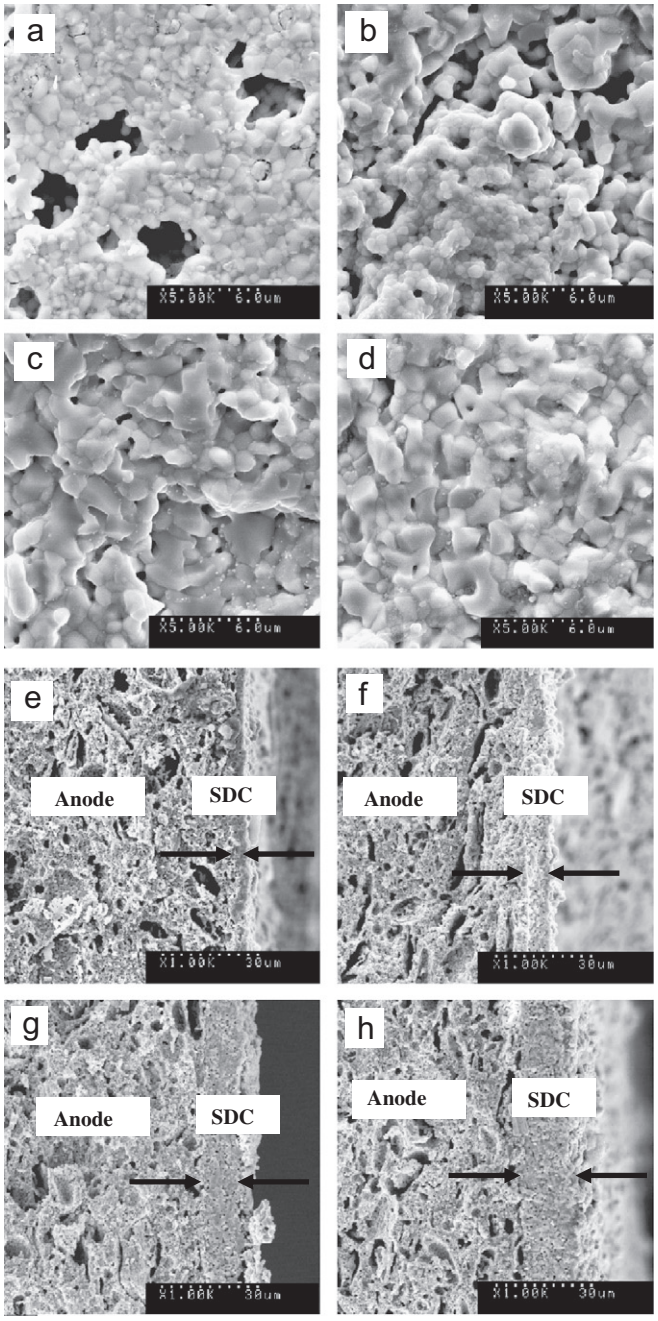

Fig. 1. SEM result for surface views of SDC films with the printing times of 1 (a), 3 (b), 5 (c), and 7 (d), and cross-sectional views of single cells with the printing times of 1 (e), 3 (f), 5 (g), and 7 (h).

The dependence of OCV of the cells measured at 600 °C on the printing times was plotted in Fig. 3. As shown in Fig. 3, when the printing times was below 5, the OCV exhibited a linear increase. When the printing times was beyond 5, the OCV slightly increased to 0.82 V. This value was close to the upper limit of OCV of single cell with SDC electrolyte.

I–V and *I–P* curves for the single cells measured at 600 °C were plotted in Fig. 4. As shown in Fig. 4, the two single cells with SDC electrolyte film fabricated by

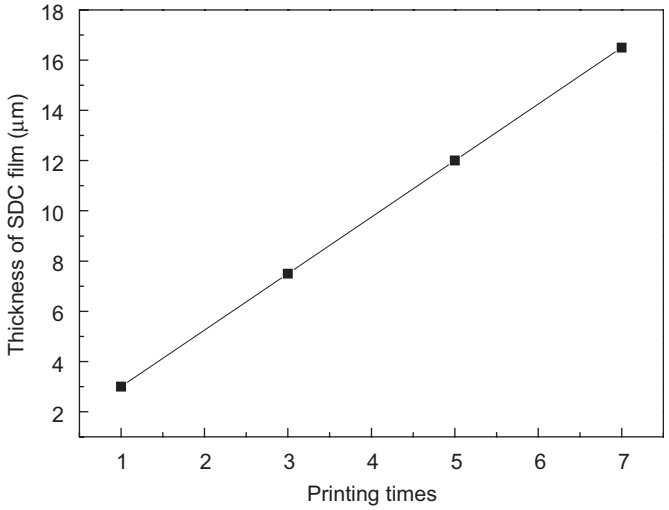

Fig. 2. Dependance of thickness of SDC films on printing times.

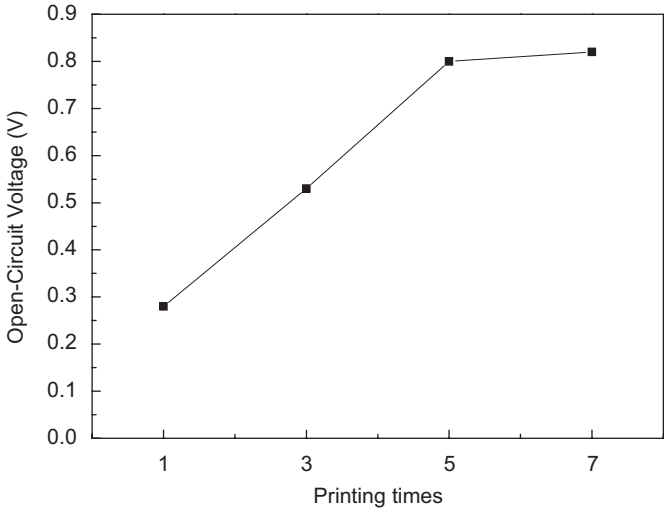

Fig. 3. Dependance of OCV (open-circuit voltage) of single cells on printing times at 600 °C.

one- and three-time printing exhibited not-stable performance and some data points were greatly away from the trend with their OCVs very low. This result was attributed to the gas cross-leakage of SDC electrolyte film. The cell with SDC film fabricated by seven-time printing processing exhibited the highest power density of about 0.5 W/cm^2.

Although it is possible to slightly increase the OCV by further increasing the printing times, the increase of printing times results in a relatively high cost for fabrication and a thicker electrolyte film, which is not advantageous to cell performance. So it can be concluded that the seven-time printing processing should be preferred during SDC film fabrication by screen-printing.

3.2. Effect of ink composition

In this section, the seven-time printing processing was adopted. Ink for screen-printing was prepared by adding

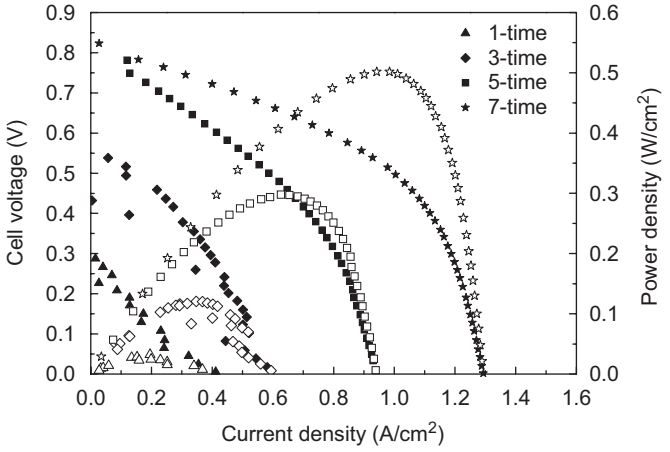

Fig. 4. *I–V* and *I–P* curves at 600 °C of single cells with the printing times of 1, 3, 5 and 7.

x wt% ($x = 30$, 40, 50, and 60) SDC powder into ethyl cellulose–terpineol vehicle.

3.2.1. SEM

Fig. 5 showed surface images of SDC films fabricated using the ink containing x wt% ($x = 30$, 40, 50 and 60) SDC powder, and cross-sectional images of single cells. As shown in the cross-sectional images in Fig. 5, all the SDC films exhibited almost the same thickness of about 16.5 μm, which indicated that screen-printing processing in this paper was reproducible. As shown in Fig. 5(e)–(h), the SDC film with $x = 40$ was dense and some cracks occurred on surfaces of the other three films. This result suggested that the ink composition had a great effect on the quality of the film. When the value of x was low, the ink contained too much organic impregnant and the impregnant was away from the green film by sintering at high temperatures, which resulted in a large amount of pores in the film as shown in Fig. 5(e). As the value of x was 50 or more, the fluidity of ink was poor and the imprint, which was produced by the terylene screen during the screen-printing processing, was not able to disappear automatically. Therefore, it was not surprising to find some cracks on the films after sintering, as shown in Fig. 5(g) and (h).

3.2.2. Cell performance

To investigate the effect of ink composition on cell performance, the dependence of OCV on the value of x, and *I–V* and *I–P* curves of single cells with $x = 30$, 40, 50, and 60 was measured at 600 °C. The result was shown in Figs. 6 and 7. As shown in Fig. 6, the cell with $x = 40$ exhibited the highest OCV of 0.82 V. The other three cells exhibited relatively low OCVs, which resulted from the gas cross-leakage, due to the bad densification of SDC electrolyte film. This result well-matched the analysis in Section 3.2.1. As shown in Fig. 7, the cell with $x = 40$ provided the highest power density of about 0.5 W/cm^2 and a short-circuit current density of about 1.3 A/cm^2. Due to their low OCVs, the other three cells with $x = 30$, 50 and 60

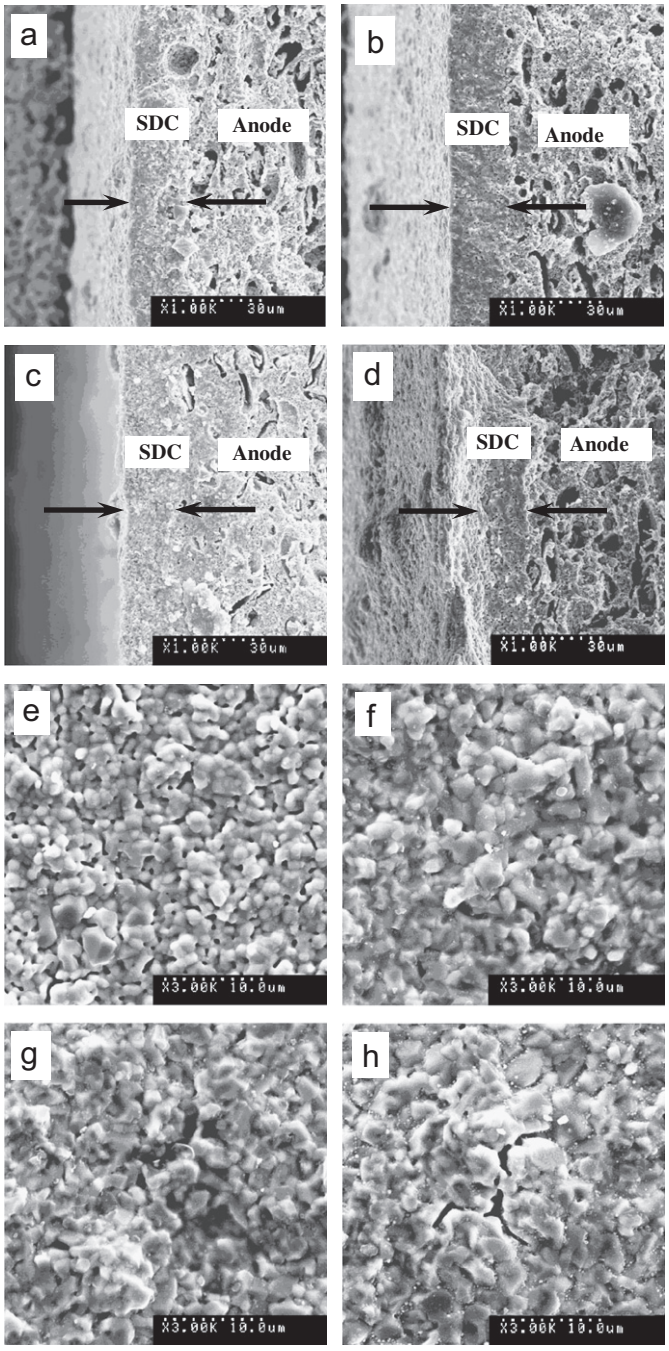

Fig. 5. SEM result for cross-sectional views of the single cells with $x = 30$ (a), $x = 40$ (b), $x = 50$ (c), $x = 60$ (d), and surface views of the SDC films with $x = 30$ (e), $x = 40$ (f), $x = 50$ (g), $x = 60$ (h). The SDC films in the single cells were fabricated by screen-printing processing, using the ink containing x wt% SDC powder.

exhibited poor output performance. So the ink containing 40 wt% SDC powder should be preferred to fabricate SDC film by screen-printing.

3.3. Effect of sintering temperature

In this section, the ink containing 40 wt% SDC powder was used to fabricate SDC films and a seven-time printing processing was adopted.

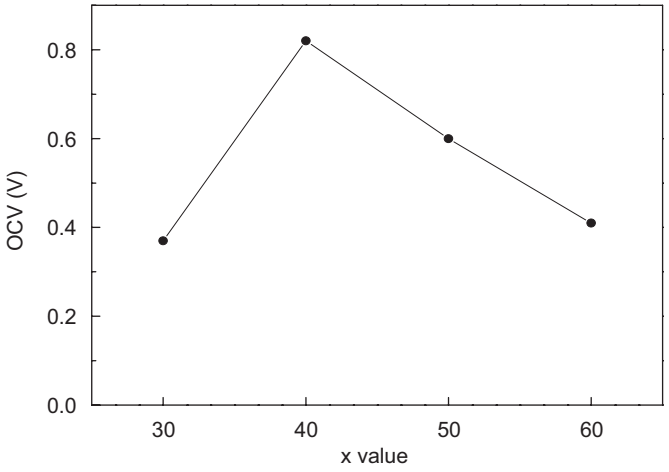

Fig. 6. OCV of single cells as a function of x value at 600 °C.

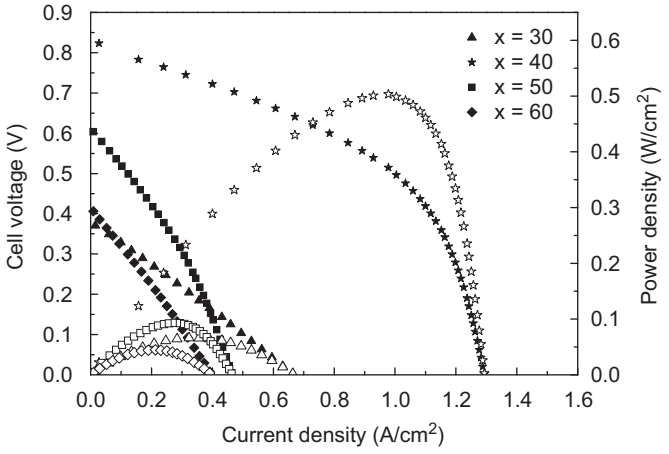

Fig. 7. *I–V* and *I–P* curves at 600 °C of single cells with $x = 30$, 40, 50, and 60.

3.3.1. SEM

Fig. 8 showed SEM result for surface views of SDC films sintered at 1300, 1350, 1400 and 1450 °C. As shown in Fig. 8, the size of grain of in SDC films increased with the sintering temperature. The two SDC films sintered at 1300 and 1350 °C exhibited porous structure, with the other two ones sintered at 1400 and 1450 °C dense. So the lowest sintering temperature, at which dense SDC films was prepared, was 1400 °C.

3.3.2. Cell performance

Fig. 9 showed OCVs of single cells with different sintering temperatures of 1300, 1350, 1400 and 1450 °C measured at 600 °C. With the increasing of sintering temperature, the OCV increase greatly in the temperature region below 1400 °C. The OCV of cell with the sintering temperature of 1400 °C was 0.82 V. However, the cell with the sintering temperature of 1450 °C exhibited an OCV of about 0.8 V, which was lower than that of the cell with the sintering temperature of 1400 °C. During the sintering

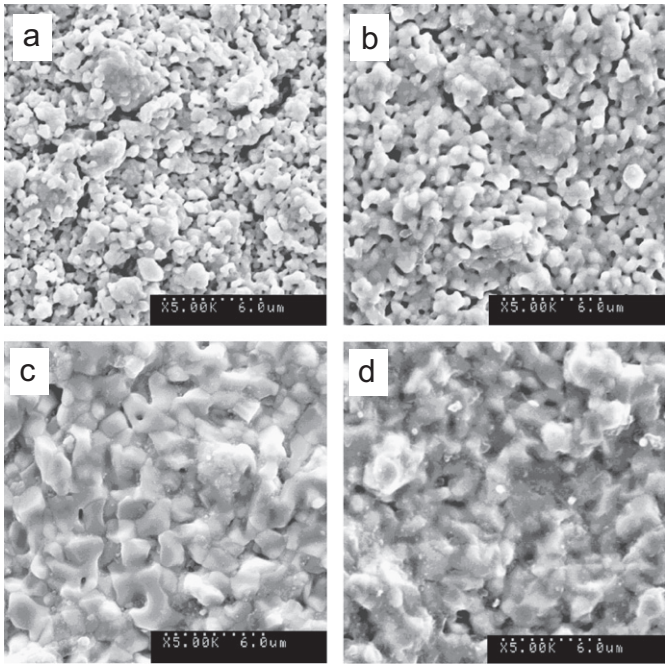

Fig. 8. SEM result for surface views of SDC films with different sintering temperatures of 1300 °C (a), 1350 °C (b), 1400 °C (c) and 1450 °C (d).

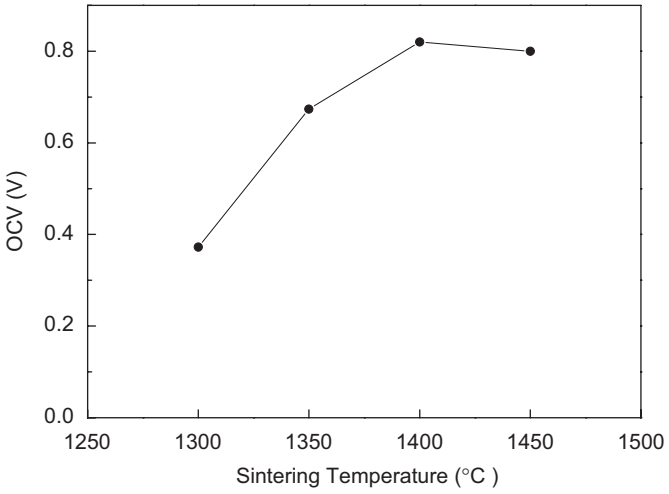

Fig. 9. OCV of single cells measured at 600 °C as a function of sintering temperature.

processing, there was stress between the electrolyte and anode substrate. When the sintering temperature for the fabrication of SDC film was increasing, the stress became more and more. If the sintering temperature was too high, the cell was cracked or broken, which resulted in a low OCV.

Fig. 10 shows the output performance of single cells with different sintering temperature of 1300, 1350, 1400 and 1450 °C measured at 600 °C. The cell with the sintering temperature of 1400 °C provided the highest power density of 0.5 W/cm^2. Low OCVs badly affected the output power

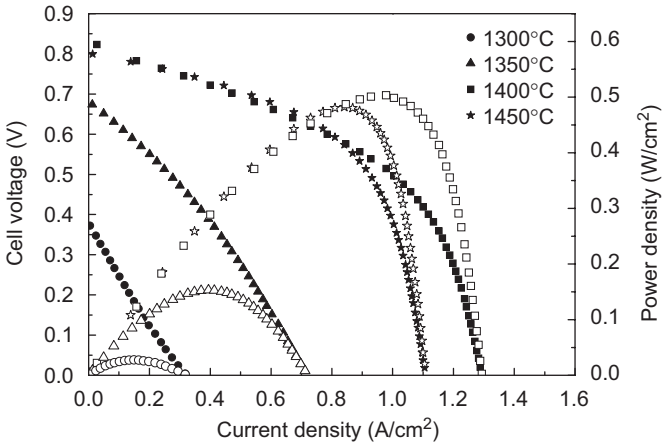

Fig. 10. *I–V* and *I–P* curves at 600 °C of single cells with different sintering temperatures of 1300, 1350, 1400 and 1450 °C.

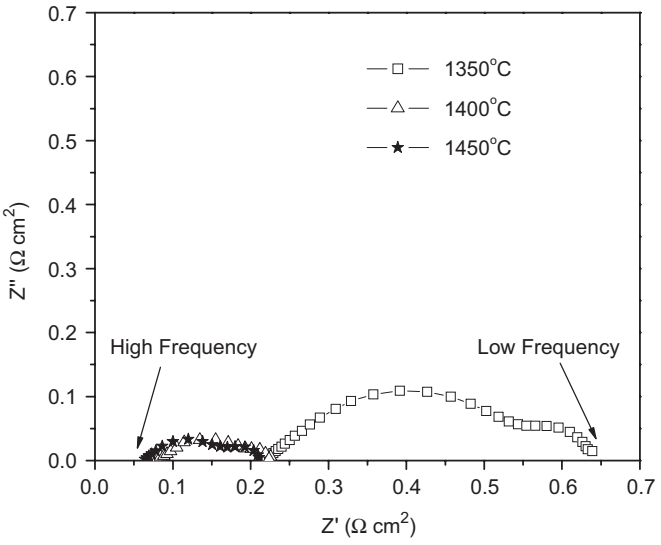

Fig. 11. Impedance spectra of single cells with different sintering temperatures of 1300 °C (a), 1350 °C (b), 1400 °C (c) and 1450 °C (d) under open-circuit condition at 600 °C.

density of the other three cells with the sintering temperature of 1300, 1350 and 1450 °C. The cell with the sintering temperature of 1450 °C exhibited a more serious concentration polarization, which resulted from the over-sintering of anode substrate during the preparation of SDC film.

Fig. 11 showed the impedance spectra of the single cells with different sintering temperatures of 1350, 1400 and 1450 °C, under open-circuit condition at 600 °C. The result for the cell with the sintering temperature of 1300 °C was not plotted here, because the data points were in a serious disorder, which resulted from the not-dense electrolyte and gas cross-leakage. As shown in Fig. 11, the intercept at high frequency on the real axis was ohmic resistance (R_o), and the difference between the two intercepts on the real

Table 1
Fitting result for Ohmic resistance (R_o), interface resistance (R_i) and total resistance (R) of the single cells with different sintering temperatures of 1350, 1400 and 1450 °C at 600 °C

	Sintering temperature (°C)		
	1350	1400	1450
R_o ($\Omega\,cm^2$)	0.22	0.08	0.064
R_i ($\Omega\,cm^2$)	0.42	0.14	0.146
$R = R_o + R_i$ ($\Omega\,cm^2$)	0.64	0.22	0.21

axis was interface resistance (R_i). The intercept at low frequency on the real axis was the total resistance (R), where $R = R_o + R_i$. The detailed fitting result for R_o, R_i and R was displayed in Table 1. The two cells with the sintering temperature of 1400 and 1450 °C exhibited almost the same interface resistance R_i, and the R_i of the cell with the sintering temperature of 1350 °C was highest, $0.42\,\Omega\,cm^2$. With the increase of the sintering temperature, the total resistance R decreased. The cell with the sintering temperature of 1450 °C exhibited the smallest ohmic resistance ($R_o = 0.064\,\Omega\,cm^2$), which resulted from the denser electrolyte film sintered at 1450 °C. In Fig. 10, the cell with the sintering temperature of 1450 °C provided a smaller absolute value of slope than the cell with the sintering temperature of 1400 °C in the region of low current density in the I–V curve. This result was related to the smaller ohmic resistance (R_o) and total resistance (R) of the cell with the sintering temperature of 1450 °C as shown in Table 1. However, the cell with the sintering temperature of 1450 °C did not showed a highest power density, due to its serious concentration polarization in the region of high current density, as shown in Fig. 10. Therefore, the optimum sintering temperature for screen-printing fabrication of SDC film was 1400 °C.

4. Conclusions

SDC electrolyte film was successfully fabricated by screen-printing. Some technical parameters for the processing were optimized: printing times, ink composition and sintering temperature. A seven or more times printing processing was necessary to obtain dense SDC films. The ink containing 40 wt% SDC powder was preferable for screen-printing. The optimum sintering temperature for the fabrication of SDC films was 1400 °C. The single cell with the optimum parameters exhibited a power density of $0.5\,W/cm^2$ and an OCV of 0.82 V at 600 °C.

Acknowledgment

The authors gratefully acknowledge the financial support from the Ministry of Science and Technology of China 863 under Contract no. 2007AA05Z139.

References

[1] N.Q. Minh, J. Am. Ceram. Soc. 76 (3) (1993) 563–588.
[2] X. Zhang, M. Robertson, C. Deces-Petit, W. Qu, O. Kesler, R. Maric, D. Ghosh, J. Power Sources 164 (2007) 668–677.
[3] Y. Liu, S. Hashimoto, H. Nishino, K. Takei, M. Mori, J. Power Sources 164 (2007) 56–64.
[4] S. Li, Z. Lu, N. Ai, K. Chen, W. Su, J. Power Sources 165 (2007) 97–101.
[5] M. Matsuda, T. Hosomi, K. Murata, T. Fukui, M. Miyake, J. Power Sources 165 (2007) 102–107.
[6] C. Jiang, J. Ma, X. Liu, G. Meng, J. Power Sources 165 (2007) 134–137.
[7] A. Subramania, T. Saradha, S. Muzhumathi, J. Power Sources 165 (2007) 728–732.
[8] D. Lee, J.-H. Han, Y. Chun, R.-H. Song, D.R. Shin, J. Power Sources 166 (2007) 35–40.
[9] M. Kawano, H. Yoshida, K. Hashino, H. Ijichi, S. Suda, K. Kawahara, T. Inagaki, Solid State Ion. 177 (2006) 3315–3321.
[10] J.L.M. Rupp, L.J. Gauckler, Solid State Ion. 177 (2006) 2513–2518.
[11] L. Jia, Z. Lu, X. Huang, Z. Liu, Z. Zhi, X. Sha, G. Li, W. Su, Ceram. Int. 33 (2007) 631–635.
[12] C.R. Xia, M.L. Liu, Solid State Ion. 144 (2001) 249–255.
[13] X. Xin, Z. Lu, Q. Zhu, X. Huang, W. Su, J. Mater. Chem. 17 (2007) 1627–1630.
[14] J.V. Herle, R. Ihringer, R.V. Cavieres, L. Constantin, O. Bucheli, J. Eur. Ceram. Soc. 21 (2001) 1855–1859.
[15] K.W. Chour, J. Chen, R. Xu, Thin Solid Films 304 (1997) 106–112.
[16] P.K. Srivastava, T. Quach, Y.Y. Duan, R. Donelson, S.P. Jiang, F.T. Ciacchi, S.P.S. Badwal, Solid State Ion. 99 (1997) 311–319.
[17] W.S. Jang, S.H. Hyun, J. Mater. Sci. 37 (2002) 2535–2541.
[18] C.H. Wang, W.L. Worrel, S. Park, J.M. Vohs, R.J. Gorte, J. Electrochem. Soc. 148 (8) (2001) A864–A868.
[19] P. Charpentier, P. Fragnaud, D.M. Schleich, E. Gehain, Solid State Ion. 135 (2000) 373–380.
[20] J. Liu, W. Liu, Z. Lu, L. Pei, L. Jia, L.Y. He, W.H. Su, Solid State Ion. 118 (1999) 67–72.
[21] K. Chen, Z. Lu, N. Ai, X. Huang, Y. Zhang, X. Ge, X. Xin, X. Chen, W. Su, Solid State Ion. 177 (2007) 3455–3460.
[22] J. Wang, Z. Lu, X. Huang, K. Chen, N. Ai, J. Hu, W. Su, J. Power Sources 163 (2007) 957–959.
[23] Y. Zhang, X. Huang, Z. Lu, Z. Liu, X. Ge, J. Xu, X. Xin, X. Sha, W. Su, J. Power Sources 160 (2006) 1065–1073.
[24] Y. Zhang, X. Huang, Z. Lu, Z. Liu, X. Ge, J. Xu, X. Xin, X. Sha, W. Su, J. Power Sources 160 (2006) 1217–1220.
[25] X. Ge, X. Huang, Y. Zhang, Z. Lu, J. Xu, K. Chen, D. Dong, Z. Liu, J. Miao, W. Su, J. Power Sources 159 (2006) 1048–1050.
[26] I. Riess, M. Godickemeier, L.J. Gauckler, Solid State Ion. 90 (1996) 91–104.
[27] M. Godickemeier, L.J. Gauckler, J. Electrochem. Soc. 145 (1998) 414–421.